Available online at www.sciencedirect.com
ScienceDirect
Journal of the European Ceramic Society 31 (2011) 2867–2875
www.elsevier.com/locate/jeurceramsoc

Preparation and characterization of photocatalytic titania–alumina composite membranes by sol–gel methods

Ali Akbar Habibpanah, Sepideh Pourhashem, Hossein Sarpoolaky *

Department of Material Science and Engineering, Iran University of Science and Technology, Tehran, Iran

Received 21 November 2010; received in revised form 7 June 2011; accepted 24 June 2011
Available online 5 August 2011

Abstract

Titania–alumina composite membranes containing 10 and 20 mol% alumina were prepared by two different sol–gel methods; co-hydrolysis and separately peptized. The samples were characterized by different techniques. XRD results showed that for the composite membranes the anatase to rutile transformation temperature was increased by 200 and 300 °C. According to specific surface area results, alumina effectively increased the specific surface area of composite membranes compared to pure titania membranes. Microstructure of composite supported membranes was considered by scanning electron microscopy and showed a crack-free layer with 1 μm thickness. The photocatalytic activity of composite samples showed that alumina addition up to an optimum amount can slightly affect the photocatalytic activity of titania.

Keywords: Titania–alumina; Sol–gel process; Composite membranes; Photocatalytic activity

1. Introduction

Nowadays water pollution, caused by hazardous organic chemicals used by industry and agriculture, is a very serious problem. Membrane separation processes have already shown to be competitive with other separation processes for what concerns energy costs, material recovery, reduction of the environmental impact and achievement of integrated processes with selective removal of some components. However, this technique only transfers pollutants from a phase to another and only displays a simple separation function.[1–4]

On the other hand, photocatalysis is a promising technology for the purification of pre-treated and non-biodegradable wastewater. Photocatalysts have been widely used for the decomposition of harmful compounds in environment. Photocatalytic reactions allow in many cases a complete degradation of organic pollutants in very small and innoxiously species, without using chemicals, avoiding sludge production and its disposal.[5,6]

New emerging technologies permit both the reduction of the global environmental impact and the use of chemicals in treatment processes. The coupling of a photocatalytic reaction with a membrane separation process could take advantage of the synergy of both technologies resulting in a very powerful system, with the membrane having the simultaneous task of supporting the photocatalyst as well as acting as a selective barrier for the species to be degraded.[2,6–8]

Among different materials utilized for membrane and photocatalytic applications, titania ceramics are the most attractive materials due to their unique properties like high chemical stability, defouling properties, high liquid flux and high photocatalytic activity, non-environmental impact, and low cost, acting as a catalyst and being a semi-conductor. So, titania membranes are being used in different applications such as water and waste water desalination.[9–14]

Although titania has been known the most effective material in separation and photocatalysis procedures, the relatively low surface area and the poor stability of the titania structure at high temperatures (i.e. instability of anatase structure) are disadvantages.[15–18] Therefore, much attention has been paid to applications of mixed oxides containing TiO_2. A gamma alumina (produced by sol–gel) is thermally more stable (transformation temperature to alpha is around 900 °C) but it is chemically less stable then TiO_2. The mixed oxides of TiO_2 and

* Corresponding author. Tel.: +98 21 77459151; fax: +98 21 77240480.
E-mail addresses: a.habibpanah@gmail.com (A.A. Habibpanah), Sepideh_pourhashem@yahoo.com (S. Pourhashem), hsarpoolaky@iust.ac.ir (H. Sarpoolaky).

0955-2219/$ – see front matter © 2011 Elsevier Ltd. All rights reserved.
doi:10.1016/j.jeurceramsoc.2011.06.014

Al_2O_3 seem to be a good alternative to overcome the problems of the single phases like retardation of anatase to rutile transformation temperature and stabilization of porosity structure would be obtained at high temperatures.[19–22]

The goal of this research is synthesis and characterization of titania–alumina composite membranes via two different sol–gel methods and several approaches were utilized to investigate the optimum conditions of preparing stable composite sols, layer deposition, drying and calcination of the layer. Also, their photocatalytic activity as well as the effect of alumina addition on thermal stability of titania composite membranes were considered.

2. Experimental

In this research, titania–alumina composite were made by coating a single composite titania–alumina top layer (derived from composite sol) on alumina supports. Titania–alumina composite layer containing 10 and 20 mol% alumina, noted as A10-T90 and A20-T80 were prepared by sol–gel process. Two different methods were considered for preparation of the composite sols; co-hydrolysis (CH) and separately peptizing sol–gel procedure (SP).

2.1. Sol preparation

2.1.1. Separately peptizing sol–gel process

First, titania colloidal sol was prepared by hydrolysis and condensation of titanium-tetra-isopropoxide (TTIP, Merck) as a precursor.[23] It should be noticed that in order to prepare stable titania colloidal sol, an excess amount of H_2O ($[H_2O]/[Ti] > 4$) was added. A solution of titanium alkoxide in isopropanol and a solution of deionized water in isopropanol were prepared separately and the first solution was added drop wisely to the second one while stirring at high speed. The resultant product of hydrolysis was filtered and washed by deionized water to remove the excessive alcohol. Then, it was dispersed in deionized water in order to prepare a colloidal sol with Ti concentration of 0.25 mol/l, the sol was peptized by HNO_3 and also pH was adjusted. In the next step, the prepared sol was kept at 80–85 °C for 24 h while refluxing. Then, the sol was treated ultrasonically for 2 h to break the weakly agglomerated particles. Finally, the stable semi-transparent and bluish titania colloidal sol was prepared.

Alumina tri-sec-butoxide was used as a precursor for synthesis of colloidal alumina sol.[24] Aluminium alkoxide was added to deionized water heated above 80 °C while stirring and the solution was kept at 90 °C for 1 h. Then, the additional water was removed by heating the prepared sol in an open reactor and after the vaporization of alcohol, an excess amount of water was added leading to a sol with Al concentration of 0.5 mol/l. The sol was peptized by addition of HNO_3 and then was kept at 90–100 °C about 16 h under reflux condition. Finally, the synthesized sol was kept for 2 h in ultrasonic bath.

One of the methods of preparing composite sol is separately peptizing sol–gel (SP) procedure. In this way, the stable composite sols were prepared by physical mixing of the individual titania and alumina sols.[23] Stable composite sols were prepared with two different compositions of A10-T90 (SP) and A20-T80 (SP). These composite sols were prepared by mixing individual titania and alumina sols in certain ratio. After mixing the prepared titania and alumina sols, the composite sol was stirred for 2 h at room temperature. It was peptized by HNO_3 to obtain a stable sol free from agglomerates. Finally, the composite sol was put into an ultrasonic bath for 2 h.

2.1.2. Co-hydrolysis sol–gel process

The second method of preparing composite sol is co-hydrolysis (CH) procedure. In this way, the TiO_2–Al_2O_3 composite sol was prepared by co-precipitation sol–gel process with two different chemical compositions of A10-T90 (CH) and A20-T80 (CH). Composite co-hydrolyzed sols with the mentioned chemical composition were prepared by adding alumina tri-sec-butoxide to isopropanol heated to a temperature about 65 °C in a closed vessel and were stirred for about 15 min. Then, the temperature of the prepared solution was slowly reduced. Also a solution of titanium tetra-isopropoxide in isopropanol while stirring for about 15–20 min was prepared. The co-precipitation was achieved by adding slowly the solution of titanium alkoxide in isopropanol to the first prepared solution while stirring vigorously. The prepared sol was kept under heating at 80–85 °C for a few hours to evaporate its alcohol. The solution was electrostatically stabilized and peptized by HNO_3, followed by 24 h refluxing and then, keeping in an ultrasonic bath.

2.2. Powder synthesis

After both sol preparations, the composite sol was poured in a Petri-dish and the nonsupported gel layers were dried at room temperature for 24 h and then, dried at 60 °C for 3 h. The obtained gel layers were calcined at different temperatures (400–900 °C) for 1 h by heating rate of 5 °C/min. These nonsupported membranes were used for XRD and BET analyses.

2.3. Membrane preparation

In order to prepare alumina substrates, Al_2O_3 granular powder (KMS-92, Martinswerk) without any additives were pressed uniaxially into a disk of 15 mm in diameter and 2 mm in thickness to prepare alumina substrates. The disks were pressed under the pressure of 31 Mpa and were sintered at 1350 °C for 1 h.[4]

The membrane layer was formed by dip-coating the support in the prepared sol. In order to make a crack-free top layer on alumina substrates, a solution of hydroxypropyl cellulose (HPC, Aldrich, 435007) with an average molecular weight of 80,000 (0.35 g/100 ml H_2O) and polyvinyl alcohol (PVA, Acros, 821038) with molecular weight of 88,000 (0.1 g/100 ml H_2O) were added to the dipping sol as binders before coating the alumina support. To achieve the optimum condition, different amounts of mentioned additives, dipping time (5 and 10 s) and also repetition of coating procedure were examined. It must be mentioned that after every dipping and coating step, the prepared

layer was dried and calcined at optimum derived condition. The coated samples were dried for 48 h at room temperature in a relatively wet environment and then dried for 3 h at 40 °C in a relatively wet environment. After drying supported membranes, they were calcined at the optimum temperature resulted from XRD analysis for 1 h by heating rate of 10 °C/h. So, the A10-T90 and A20-T80 supported membranes were calcined at 650 and 750 °C, respectively.

Also, in order to measure photocatalytic activity of synthesized membranes, titania and composite sols were coated on borosilicate glasses (with dimensions of 15 × 10 × 2.5 mm) and dried at room temperature and calcined at 450 °C for 1 h; because of glass deformation, higher calcination temperatures were avoided.

2.4. Characterization

Different techniques were used to identify the characteristics of synthesized samples. Physical properties of alumina support were determined by Archimedes method according to ASTM 373-88 standard. The mechanical strength of the support was measured by SANTAM, STM-400 according to three-point bend test. Average pore size of substrate was evaluated by gas permeability data relating to pure Knudsen and pure Poiseuille flow regimes.

Particle size and size distribution of prepared sols were determined by zeta sizer method (Malvern DTS). The crystal structure of the membrane top layer and the effect of alumina on titania phase transformation temperature during the calcination process were identified by X-ray diffraction technique with Cu Kα wavelength (XRD, Jeol8000 diffractometer). Surface and cross section quality of the membrane layer were examined by using scanning electron microscopy (SEM, VEGA II, Tescan) and via this method, layer thickness was also determined. N_2-sorption measurement (BET, Gemini, USA, Micrometrics) was utilized to measure specific surface area and pore size of non-supported membranes.

2.5. Photocatalytic activity of titania and titania–alumina composite membranes

The photocatalytic activity of the prepared titania and titania–alumina composite membranes coated on alumina substrates and borosilicate glasses was measured by the photocatalytic degradation of green malachite in an aqueous solution. Titania and titania–alumina composite membranes were placed on a Petri-box containing 10 ml of 5 ppm aqueous solution of green malachite. The Petri-box was placed in a homemade box. Then, the membrane was irradiated by a UV source (Osram, 360–415 nm) which has the maximum intensity of 370 nm close to the anatase band gap. After UV-radiation, the concentration of green malachite solution was examined by UV–visible spectrophotometer (Shimazu, UV-1700 series). Concentration changes of green malachite were measured in presence of the titania and titania–alumina composite membrane as a function of time.

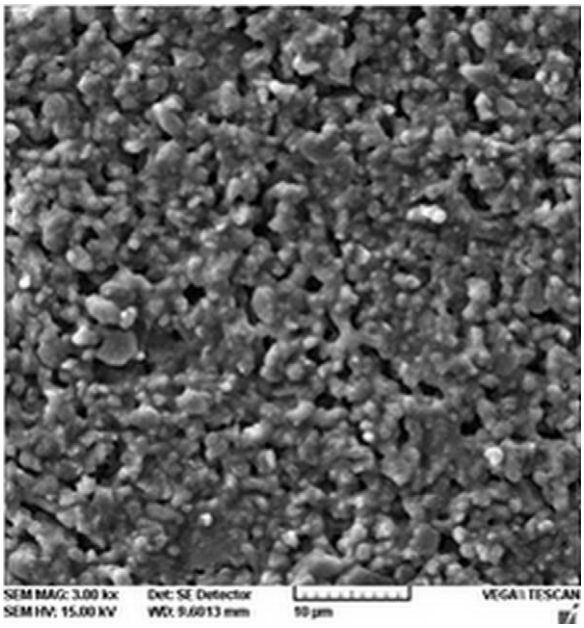

Fig. 1. SEM surface image of α-Al_2O_3 support, sintered at 1350 °C for 1 h.

3. Results and discussion

3.1. Support

Fig. 1 shows SEM surface image of the α-Al_2O_3 support, sintered at 1350 °C for 1 h and the calculated average pore diameter versus sintering temperature using equations and data relating to gas permeability pertaining to pure Knudsen and pure Poiseuille flow regimes[1] is given in Fig. 2 Average pore sizes according to SEM and gas permeability data are between 1–3 μm and 0.16–0.195 μm, respectively and there is a significant difference between them. Falamaki et al.[25] determined the pore size of alumina and zirconia support via different methods like wet permeability tests, SEM, gas permeability data pertaining to pure Knudsen and pure Poiseuille flow regimes. They resulted that the maximum permeable pore size so determined is not always equal to the maximum pore size due to SEM micrographs. Also, they observed that, in the case of alumina, the calculated pore diameters according to gas permeability data pertaining to pure Knudsen and pure Poiseuille flow regimes are less than half the

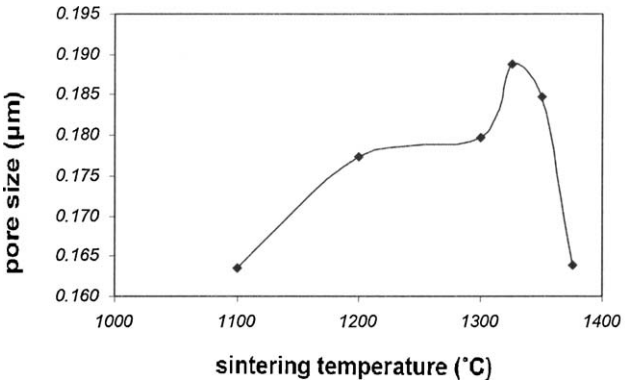

Fig. 2. Calculated pore diameter versus sintering temperature.

Table 1
Optimum conditions for the preparation of stable sols.

Type of sol	Titania	Alumina	Composite (CH)	Composite (SP)
$[H_2O]/[Ti]$	25	100	150	–
$[H^+]/[Ti]$	0.5	0.07	0.5	–
pH	1.5	4	1	2
Peptization temperature (°C)	80–85	85–90	80–85	–
Peptization time (h)	24	24	24	–

values obtained for the mean flow pore size. As it can be resulted, the SEM micrographs only show the maximum pore size, but the mean flow pore size and pore diameters can be calculated by mentioned methods and the results of SEM is significantly different from the others.[25]

Alumina was chosen as a support due to high chemical stability in acidic and basic environment. Its sintering temperature should be chosen in a way that the synthesized membrane gives both desired strength and permeability.[26,27] According to the results of strength, porosity and firing shrinkage, the optimum sintering temperature of the support was chosen 1350 °C.

3.2. Sol preparation

Table 1 shows optimum conditions of preparing stable colloidal sols and results of zeta sizer are presented in Table 2. Optimum pH for colloidal titania sol, alumina sol, composite sol via co-hydrolysis and separately peptizing sol–gel process are different from one another. According to Table 2, comparison of the composite sol with pure titania one shows that the smallest particle size is for titania colloidal sol which has the average particle size of 29.5 nm and the minimum size of 10.1 nm. In comparison, A20-T80 (SP) composite sols have the largest particle size distribution, with the mean particle size of 40.1 nm and the minimum size of 15.7 nm. Therefore, presence of alumina makes the particle sizes larger. Results of zeta sizer indicate that all samples showed a narrow particle size distribution revealing that the conditions of sol preparation were optimum and satisfactory. According to the results, by comparison of CH and SP sol–gel methods, although their particle size and particle size distribution do not have significant difference, SP sol gives slightly larger mean particle size and broader particle size distribution.

Small particle size and narrow particle size distribution are desired parameters for layer formation by sol on the substrate; therefore, after calcination, small pore size and narrow pore size distribution will be obtained.[24,28]

To prepare a stable sol, control of peptization parameters like pH and temperature are important. In peptization step, agglomerated particles will be scattered and a layer of H^+ surrounds particles or a small group of particles and prevents agglomeration via repulsive forces due to electrical double layer. Amount of pH for every stable sol is different. Therefore, with increasing pH from optimum condition, sol particles will be flocculated due to attractive forces between particles. On the other hand, if pH is lower than the optimum level, ion concentration in electrical double layer will increase; therefore, the electrical double layer will compact and the result will be sol precipitation.[15,24,28,29]

Consequently, if peptization temperature is lower than optimum temperature, peptization step will be prevented and by increasing temperature, sol particles can overwhelm the energy barrier of coagulation via their thermal energy and a reversible coagulation takes place.

Table 2
Zeta sizer results of prepared sols.

Type of sol	Mean particle size (nm)	Minimum particle size (nm)
Titania	29.5	10.1
A10-T90 (CH)	38.5	11.7
A20-T80 (CH)	35.2	13.5
A20-T80 (SP)	40.1	15.7

3.3. Phase analysis

Fig. 3 shows XRD pattern of unsupported titania membranes calcined for 1 h at different temperatures. It shows that pure titania until 450 °C is fully crystalline and the major stable phase in pure titania sample is only anatase but increasing temperature above 500 °C causes anatase-to-rutile phase transition. So, rutile phase is stabilized by increasing temperature.

The diffraction pattern of composite titania membranes as a function of calcination temperature are plotted in Figs. 4 and 5. It must be mentioned that because XRD patterns of CH and SP samples were similar, only CH XRD patterns are presented. As shown in Fig. 4, the amount of anatase phase for A10-T90 samples increases by increasing temperature up to 650 °C and at this

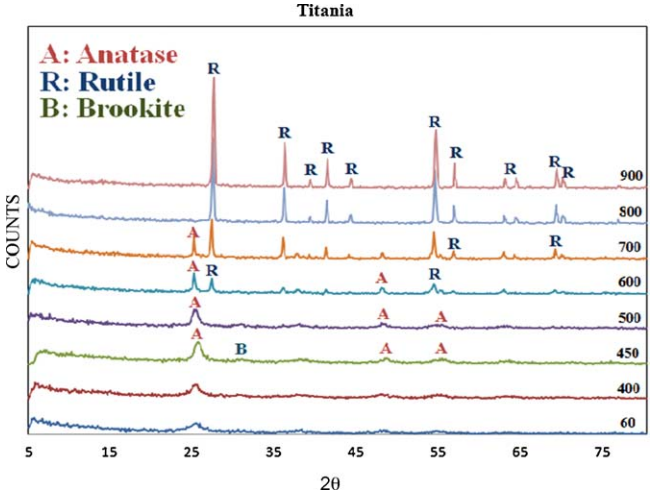

Fig. 3. XRD patterns of titania powder, calcined for 1 h at 60, 400, 450, 500, 600, 700, 800 and 900 °C. A: anatase and R: rutile.

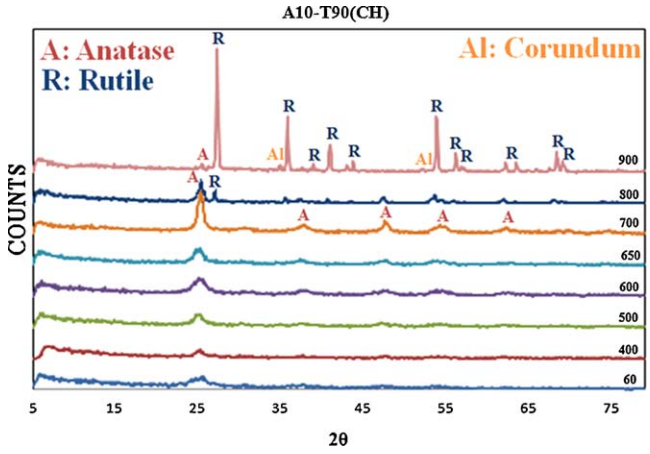

Fig. 4. XRD pattern of A10-T90 (CH) powder, calcined for 1 h at 60, 400, 500, 600, 650, 700, 800 and 900 °C. A: anatase, R: rutile and Al: corundum.

temperature, the mentioned samples have the most anatase quantity. At 700 °C, the rutile phase appears and the amount of anatase phase decreases via increasing temperature. At higher temperatures, the only stable phase of titania is rutile. On the other hand, A20-T80 samples show rutile phase formation from 800 °C. So, in composite titania–alumina unsupported membranes containing 10 mol% and 20 mol% alumina, compared with pure titania ones, anatase to rutile phase transformation is retarded about 200 and 300 °C, respectively. In all samples, the prepared powders are amorphous after drying and transform from amorphous to crystalline anatase phase via increasing temperature.

The crystallite sizes of prepared unsupported membranes calcined at different temperatures were determined by Scherer's equation.[30] Crystallite sizes of unsupported membranes calcined at different temperatures for 1 h are shown in Fig. 6. As the figure shows, the crystallite size is increased by increasing temperature. The crystallite size of titania changes abruptly from 500 °C due to anatase–rutile phase transformation, but composite samples show broader temperature range with the least changes in crystallite size and the temperature of sudden changes in crystallite size of A10-T90 and A20-T80 samples is 700 and 800 °C, respectively. Therefore, the anatase to rutile transition

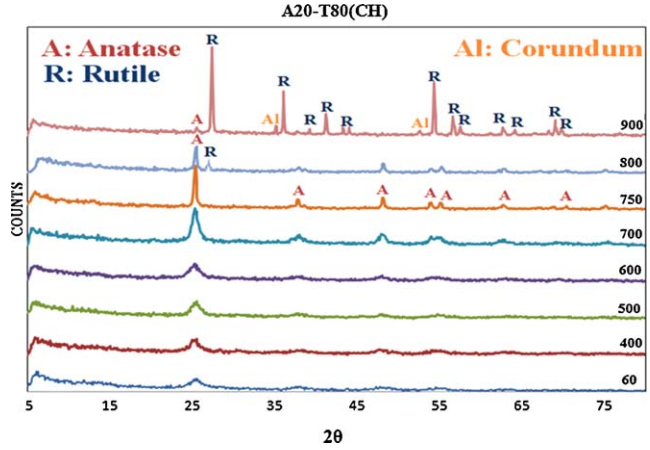

Fig. 5. XRD patterns of A20-T80 (CH) powder, calcined for 1 h at 60, 400, 500, 600, 700, 750, 800 and 900 °C. A: anatase, R: rutile and Al: corundum.

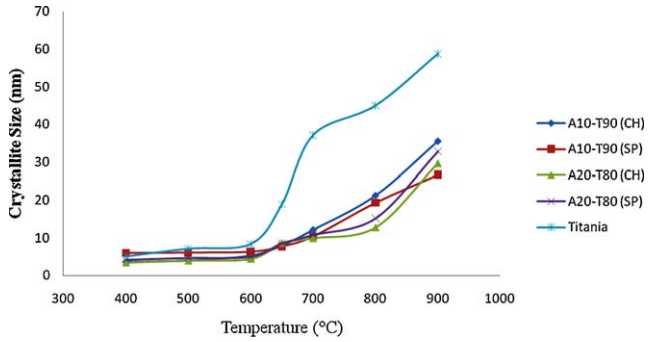

Fig. 6. Crystallite size changes according to temperature for (a) pure titania, (b) A10-T90 (SP), (c) A10-T90 (CH), (d) A20-T80 (SP), (e) A20-T80 (CH) calcined at different temperatures.

temperature is retarded and this transformation occurs at higher temperatures.

So, the optimum calcination temperature of pure titania, A10-T90 and A20-T80 composite membranes is selected 450, 650 and 750 °C for 1 h, respectively; because at these temperatures, the anatase–rutile phase transformation is prohibited, anatase is the main phase of titania and titania has a crystalline structure. Also, the crystallite size of anatase is minimized and the specific surface area is maximized.

Table 3 shows the crystallite size of unsupported membranes calcined at their optimum calcination temperatures. Crystallite sizes of pure titania and composite titania–alumina unsupported membranes are in the range of 8–10 nm and although calcination temperatures of composite samples A10-T90 and A20-T80, compared with pure titania samples, are increased, the crystallite sizes have not changed significantly. This represents that alumina has an important role in retarding anatase to rutile phase transformation and improving crystallite size.

Bosc et al.[31] reported that the optimum crystallite size for anatase in order to get the highest possible photocatalytic activity is in the range of 8–10 nm. This is because a very small crystallite size causes a shift in the light absorption spectrum and favors surface recombination of the photo-exited holes and electrons while a larger crystallite size exhibits lower surface area and thus a smaller number of catalytic active sites per unit mass of catalyst.[32–34] Crystallite size of pure titania and composite titania–alumina unsupported membranes are in the mentioned range and are appropriate. A high photocatalytic activity, broader thermal stability temperature range with minor structural changes will be expected.

Different results are reported about phase transition temperature and thermal stability of titania[34–36,17] and composite titania–alumina.[17,37–40] At temperatures lower than anatase to rutile phase transformation, the structural changes have not occurred yet and crystallite size growth of anatase is small. By increasing temperature, anatase to rutile phase transformation occurs which is accompanied by 8% volume shrinkage.[41] Also, the rate of crystallite growth becomes faster. So, specific surface area and porosity decrease. On the other hand, these changes result additional stresses in layer formation and cracks are formed. So, anatase–rutile phase transformation must be prevented.[24,28,42]

Table 3
Crystallite size of titania and composite samples at optimum calcination temperature.

Sample	Titania (450 °C)	A10-T90 (SP-650 °C)	A10-T90 (CH-650 °C)	A20-T80 (SP-750 °C)	A20-T80 (CH-750 °C)
Crystallite size (nm) (±0.01)	7.19	8.25	8.01	10.08	9.98

Anatase to rutile phase transformation take place by coalescence of small anatase particles into larger rutile grains and is accompanied by considerable grain and pore growth. A lower sub-coordination number leads to a situation in which anatase particles have a lower number of contact points which decreases the probability of their coalescence into larger rutile particles.[32,43]

Oxygen vacancy concentration in the anatase structure due to the presence of substitutional or interstitial ions in the crystal lattice changes the anatase–rutile transformation temperature. It has been reported that Al^{3+} ions accelerate the transition of anatase to rutile phase due to their smaller radius and lower valence than Ti^{4+} ions. Therefore, the oxygen vacancy concentration may be increased, but it must be noted that oxygen vacancy is not the only reason of anatase stability. When cations are introduced in TiO_2 matrix interstitially, they will fill the empty space in the matrix and reduce the atomic mobility of anions and cations and make the anatase phase more stable. When the size of the dopants increases, they will fit more tightly into these interstices and the stability of the phase will increase.[15,43–45]

The metastable anatase solid solution containing alumina was formed at temperatures lower than 900 °C and active sites will be made in anatase structure. Also, stabilizing improves when metallic ions enter titania structure. Therefore, alumina additive might incorporate in anatase lattice to form anatase solid solution rather than just staying on the surface of titania particles. Distribution of alumina on the surface of titania particles and increasing activation energy of rutile nucleation on titania–alumina surface retards the anatase to rutile phase transformation. Due to limited solubility of alumina in rutile, by increasing temperature above 900 °C, small amount of alumina comes out of titania structure in form of α-Al_2O_3; i.e. α-Al_2O_3 can be directly formed from the exsolution of the mentioned anatase solid solution.[17,37]

3.4. BET surface area and pore structure

Table 4 shows the results of specific surface area and mean pore size of unsupported membranes. Results indicate that the pore size of pure titania and A10-T90 layers is in the mesoporous range according to IUPAC Standard. As is shown in Table 4, titania samples have lower specific surface area and larger pore size and addition of alumina increases the specific surface area and reduces the pore size and CH procedure gives higher surface area and lower pore size than SP method. This is due to morphology promotion behavior of alumina for titania.

Table 4
N_2-adsorption characteristics of titania and titania–alumina samples calcined at 450 °C for 1 h.

Sample	S_{BET} (m^2/g)	Mean pore size (nm) (±0.01)
Titania	87.4	4.22
A10-T90 (SP)	175.35	4.0
A10-T90 (CH)	186.29	3.30

3.5. Microstructural study

Fig. 7 shows surface and cross section of the supported composite membrane A10-T90 (CH). As it is obvious from the image, a smooth and crack-free composite layer on top of the alumina support is formed and the thickness of the top layer is about 1 μm.

In this research, various sol concentrations of composite sols were prepared and different amount of organic additives and different coating times were being utilized to achieve the optimum conditions for preparing a crack-free membrane. Results show that beside careful selection of processing conditions, sols with lower concentration and shorter dipping time (5 s) can lead to a crack-free membrane. Although other researchers mentioned that addition of PVA is sufficient for dipping composite solution,[23,46] in this work, addition of PVA did not lead to a crack-free layer and the best result were achieved by addition of both HPC and PVA organic additives to the dipping solution; because the prepared composite sols had a large quantity of titania. Appropriate calcination temperature according to XRD results and maintaining titania in anatase phase is another reason for having crack-free membranes.

It is pretty important to control layer thickness in membranes which has a significant effect on membrane permeability and by increasing membrane thickness, its permeability decreases. So, obtaining optimum thickness is necessary. Optimum thickness of top layer for membranes is about 1–2 μm. If the layer thickness is more than an optimum amount, cracks will be made during drying and calcination steps. Also, optimum thickness will provide better photocatalytic activity and will overcome the irregularities and roughness of the support surface. If layer thickness is not sufficient, it must be increased via increasing sol concentration and dipping time or multi dipping technique must be utilized.[15,20,23,47,48,26]

3.6. Photocatalytic properties

Table 5 compares the photoactivity of pure titania and composite titania–alumina membranes which are the average results of three separate test on each samples. A10-T90 (CH) and A10-T90 (SP) samples coated on alumina substrates calcined at 650 °C showed similar degradation of green malachite after 3 h of UV irradiation. Therefore, the synthesis method may not have great effect on the photocatalytic activity of the samples.

Table 5
The photocatalytic activity of titania and titania–alumina composite membranes.

Type of membrane	Type of support	UV irradiation time	Decomposition (%) (±1%)
A10-T90 (SP)	Alumina	After 3 h	95
A10-T90 (CH)	Alumina	After 3 h	95
Titania	Borosilicate glass	After 2 h	79
A10-T90 (CH)	Borosilicate glass	After 2 h	80
A20-T80 (CH)	Borosilicate glass	After 2 h	75

Pure titania and A10-T90 samples coated on borosilicate glasses calcined at 450 °C show 79% and 80% degradation of green malachite after 2 h, respectively. As a result, addition of 10 mol% of alumina to titania did not have any especial effect on the photocatalytic activity. On the other hand, A20-T80 samples show 75% degradation of green malachite after 2 h. Therefore, this amount of alumina addition can reduce the photocatalytic activity of titania slightly.

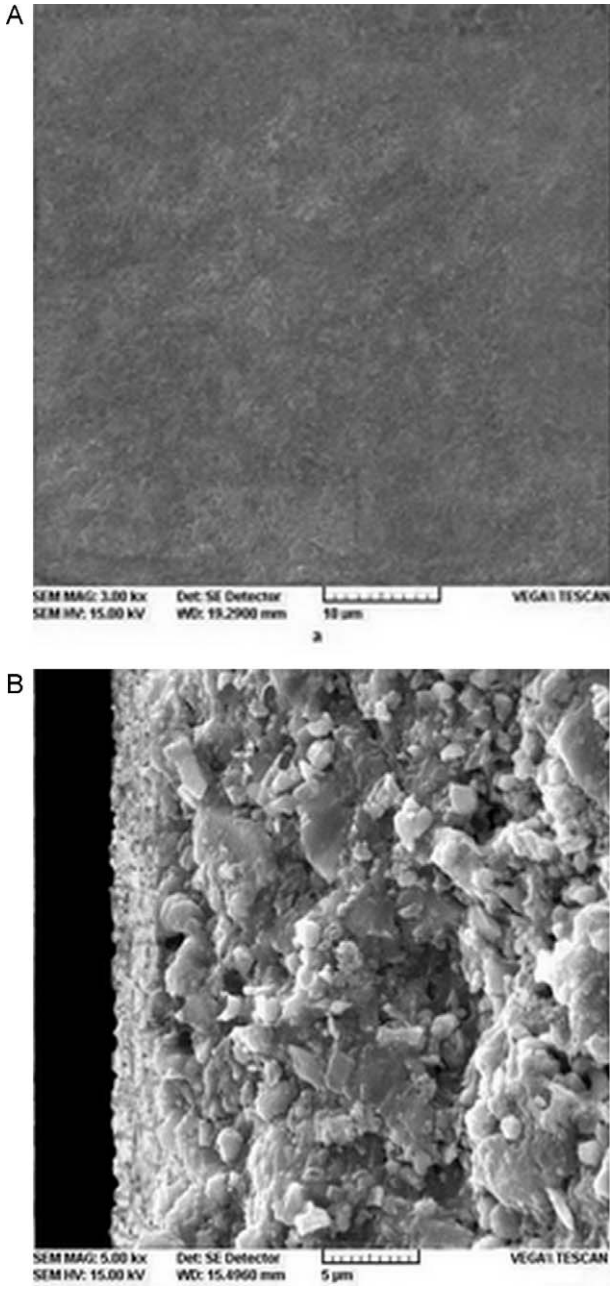

Fig. 7. SEM (a) surface and (b) cross section image of A10-T90 (CH) membrane, calcined at 650 °C for 1 h.

Titania is broadly used in photocatalytic applications due to its high photocatalytic activity. It has been reported that if Al^{3+} ions are introduced into the titania matrix substantially, they will produce a reduction in titania photocatalytic activity due to increasing oxygen deficiency; because oxygen deficiency leads to a faster rate of electron–hole recombination and therefore, reduces the photocatalytic activity. As previously discussed, alumina is mainly introduced into titania matrix interstitially and occupies interstitial sites. It must be noted that specific surface area affects the photocatalytic activity directly that maintains characteristics like amount of electron–hole recombination and number of active sites on the surface of photocatalyst. Higher specific surface area reduces the amount of charge carrier recombination via shortening the migration distance of carriers to surface and on the other hand; it increases the active sites on the photocatalytic surface, i.e. higher electron–hole recombination with surrounding will be resulted. The faster rate of electron–hole recombination with their environment is equal to the reduction of electron–hole recombination with each other and so, a higher photocatalytic activity will be obtained.[2,49–52]

4. Conclusion

Crack-free photocatalytic titania–alumina composite membranes were prepared via two different sol–gel methods; CH and SP procedures. The anatase-to-rutile transformation temperature increased 200 and 300 °C by adding 10 mol% and 20 mol% alumina to titania but the crystallite size of composite samples had not changed significantly and methods of sol preparation did not have any significant difference on phase structure. Titania and A10-T90 membranes showed mesoporous behavior and composite membranes showed higher surface area and smaller pore size and CH procedure gave the highest surface area and the lowest pore size.

In this research composite membranes were fabricated on alumina supports and the thickness of the top layer is about 1 μm. In this regard, sol preparation, inorganic additives, drying and calcination steps of membrane were important factors to avoid crack formation in microstructure.

Also, photocatalytic activity results showed that composite membranes containing 10 mol% alumina can compensate the reduction of photocatalytic activity by increasing specific

surface area but photocatalytic activity decreased slightly for samples containing 20 mol% alumina. As a result, alumina addition retarded the phase transformation of titania and increased calcination temperature without any significant effect on titania photocatalytic activity. Therefore, using titania–alumina composite membranes is a way of improving separation and photocatalytic behavior of titania membranes at high temperatures.

References

1. Li K. *Ceramic membranes for separation and reaction*. John Wiley & Sons; 2007.
2. Zhang H, Quan X, Chen S, Zhao H, Zhao Y. Fabrication of photocatalytic membrane and evaluation its efficiency in removal of organic pollutants from water. *Separation and Purification Technology* 2006;**50**:147–55.
3. Molinari R, Mungari M, Drioli E, Di Paola A, Loddo V, Palmisano L, et al. Study on a photocatalytic membrane reactor for water purification. *Catalysis Today* 2000;**55**:71–8.
4. Alem A, Sarpoolaky H, Keshmiri M. Sol–gel preparation of titania multilayer membrane for photocatalytic applications. *Ceramics International* 2009;**35**:1837–43.
5. Zeltner WA, Tompkins DT. *Shedding light on photocatalysis*. American Society of Heating, Refrigerating and Air-Conditioning, Engineers; 2005. p. 111.
6. Cui P, Zhao X, Zhou M, Wang L. Photocatalysis–membrane separation coupling reactor and its application. *Chinese Journal of Catalysis* 2006;**27**(9):752–4.
7. Molinari R, Palmisano L, Drioli E, Schiavello M. Studies on various reactor configurations for coupling photocatalysis and membrane processes in water purification. *Journal of Membrane Science* 2002;**206**:399–415.
8. Mozia S. *Separation and Purification Technology* 2010;**73**:71–91.
9. Alem A, Sarpoolaky H, Keshmiri M. Titania ultrafiltration membrane: preparation, characterization and photocatalytic activity. *Journal of the European Ceramic Society* 2009;**29**:629–35.
10. Zhang X, Dua AJ, Lee P. TiO_2 nanowire membrane for concurrent filtration and photocatalytic oxidation of humic acid in water. *Journal of Membrane Science* 2008;**313**:44–51.
11. Pagana A, Stoitsas K, Zaspalis VT. Applied pilot scale studies on ceramic membranes for the treatment of waste water systems. *Global NEST Journal* 2006;**8**:23–30.
12. Wang YH, Liu XQ, Meng GY. Preparation and properties of supported 100% titania ceramic membranes. *Materials Research Bulletin* 2008;**43**:1480–91.
13. Gaya UI, Abdullah AH. Heterogeneous photocatalytic degradation of organic contaminants over titanium dioxide: a review of fundamentals, progress and problems. *Journal of Photochemistry and Photobiology C: Photochemistry Reviews* 2008;**9**:1–12.
14. Chong MN, Jin B, Chow CWK, Saint C. Recent developments in photocatalytic water treatment technology: a review. *Water Research* 2010;**44**:2997–3027.
15. Sekulić-Kuzmanović J. Mesoporous and micro porous titania membranes, Doctoral Dissertation, University of Twente; 2004.
16. Fox MA, Dulay MT. Acceleration of secondary dark reactions of intermediates derived from adsorbed dyes on irradiated TiO_2 powders. *Journal of Chemical Reviews* 1993;**93**:341–57.
17. Jung Y-S, Kim D-W, Kim Y-S, Park E-K, Baeck S-H. Synthesis of alumina–titania solid solution by sol–gel method. *Journal of Physics and Chemistry of Solids* 2008;**69**:1464–7.
18. Tursiloadi S, Imai H, Hirashima H. Preparation and characterization of mesoporous titania–alumina ceramic by modified sol–gel method. *Journal of Non-Crystalline Solids* 2004;**350**:271–6.
19. Bae D-S, Han K-S, Choi S-H. Preparation and thermal stability of doped TiO_2 composite membranes by the sol–gel process. *Journal of Solid State Ionics* 1998;**109**:239–45.
20. Kumar K-NP, Keizer K, Burggraaf AJ. Textural stability of titania–alumina composite membranes. *Journal of Materials Chemistry* 1993;**3**(9):917–22.
21. Alem A, Sarpoolaky H. The effect of silver doping on photocatalytic properties of titania multilayer membranes. *Solid State Sciences* 2010;**12**:1469–72.
22. Yang GCC, Li C-J. Preparation of tubular TiO_2/Al_2O_3 composite membranes and their performance in electrofiltration of oxide. *Desalination* 2006;**200**:74–6.
23. Zaspalis VI, Vanpraag W, Keizer K, Ross JRH. Synthesis and characterization of primary alumina, titania and binary membranes. *Journal of Materials Science* 1992;**27**:1023–35.
24. Leenaars AFM, Keizer K, Burggraaf AJ. The preparation and characterization of alumina membranes with ultra-fine pores. *Journal of Materials Science* 1984;**19**:1077–88.
25. Falamaki C, Afarani MS, Aghaie A. Initial sintering stage pore growth mechanism applied to the manufacture of ceramic membrane supports. *Journal of the European Ceramic Society* 2004;**24**:2285–92.
26. Bhave R. *Inorganic membrane synthesis, characterization and application*. Elsevier; 1991.
27. Tsuru T, Hironaka D, Toshioka T, Asaeda M. Titania membranes for liquid phase separation: effect of surface charge on flux. *Journal of Separation and Purification Technology* 2001;**25**:307.
28. Van Gestel T, Vandecasteele C, Buekenhoudt A, Dotremont C, Luyten J, Leysen R, et al. Alumina and titania multilayer membranes for nanofiltration: preparation, characterization and chemical stability. *Journal of Membrane Science* 2002;**207**:73–89.
29. Rahaman MN. *Ceramic processing and sintering*. Marcel Dekker; 2003.
30. Cullity BD. *Elements of X-ray diffraction*. second edition Addison-Wesley; 1978.
31. Bosc F, Ayral A, Albouy P, Guizard C. A simple route for low temperature synthesis of mesoporous and nanocrystalline anatase thin films. *Journal of Chemistry and Materials* 2003;**15**:2463.
32. Nair P, Mizukami F, Okubo T, Nair J, Keizer K, Burggraaf AJ. High-temperature catalyst supports and ceramic membranes: metastability and particle packing. *Ceramics Processing* 1997;**43**:2710–4.
33. Ohman LO, Paul J. Materials aspects of titanium-doped aluminas: 14% Ti/γ-Al_2O_3/Cu and sulfide Al_2O_3–TiO_2/Ni Mo. *Journal of Materials Chemistry and Physics* 2002;**73**:242.
34. Gutierrez-Alejandre A, Trombetta M, Busca G, Ramirez J. Characterization of alumina-titania mixed oxide support. *Journal of Microporous Materials* 1997;**12**:79–91.
35. Shchukin Dmitry G, Caruso Rachel A. Inorganic macroporous films from preformed nanoparticles and membrane templates: synthesis and investigation of photocatalytic and photoelectrochemical properties. *Journal of Advanced Functional Materials* 2003;**13**:789–94.
36. Suru TT, Hino T, Yoshioka T. Permporometry characterization of microporous ceramic membranes. *Journal of Membrane Science* 2001;**186**:257–65.
37. yang J, huang YX, Ferreira JMF. Inhibitory effect of alumina additive on the titania phase transformation of a sol–gel derived powder. *Journal of Materials Science Letters* 1997;**16**:1933–5.
38. Kim J, Song KC, Foncillas S, Pratsinis SE. Dopants for synthesis of stable bimodally porous titania. *Journal of the European Ceramic Society* 2001;**21**:2863–72.
39. Kaneko EY, Pulcinelli SH, Santilli CV, Craievich AF, Chiaro SSX. Characterization of the porosity developed in a new titania–alumina catalyst support prepared by the sol–gel route, papers, international union of crystallography; 2003.
40. Cecilio AA, Pulcinelli SH, Santilli CV, Maniette Y. Improvement of the MO/TiO_2–Al_2O_3 catalyst by the control of the sol–gel synthesis. *Journal of Sol–Gel Science and Technology* 2004;**31**:87–93.
41. Kumar K-NP. Growth of rutile crystallites during the initial stage of anatase-to-rutile transformation in pure titania and in titania–alumina nanocomposites. *Scripta Metallurgica et Materialia* 1995;**32**: 873–7.
42. Wang MC, Lin HJ, Yang TS. Characteristics and optical properties of ion. (Fe3+)-doped titanium oxide thin films prepared by a sol–gel spin coating. *Journal of Alloys and Compounds* 2008;**473**:394–400.

43. Vargas S, Arroyo R, Haro E, Rodríguez R. Effects of cationic dopants on the phase transition temperature of titania prepared by the sol–gel method. *Journal of Materials Research* 1999;**14**:3932–7.
44. Okada K, Yamamoto N, Kameshima Y, Yasumoti A. Effect of silica additive on the anatase-to rutile phase transition. *Journal of the American Ceramic Society* 2001;**84**:1591–6.
45. Yang J, Ferreira JMF. On the titania phase transition by zirconia additive in a sol–gel derived powder. *Materials Research Bulletin* 1998;**33**:389–94.
46. Bae D-S, Cheong D-S, Han K-S, Choi S-H. Fabrication and microstructure of Al_2O_3–TiO_2 composite membranes with ultrafine pores. *Ceramics International* 1998;**24**:25–30.
47. Torimoto T, Ito S, Yoneyama H. Effect of adsorbent used as supports for titanium dioxide loading on photocatalytic. *Journal of Environmental Sciences & Technology* 1996;**30**:1275–81.
48. Agoudjil N, Benkacem T. Synthesis of porous titanium dioxide membranes. *Desalination* 2007;**206**:531–7.
49. Choi H, Stathatos E, Dionysiou DD. Sol–gel preparation of mesoporous photocatalytic TiO_2 films and TiO_2/Al_2O_3 composite membranes for environmental applications. *Applied Catalysis B: Environmental* 2006;**63**: 60–7.
50. Anderson C, Bard AJ. Improved photocatalytic activity and characterization of mixed TiO_2/SiO_2 and TiO_2/Al_2O_3 materials. *Journal of Physical Chemistry* 1997:2611–6.
51. Xie T-H, Lin J. Origin of photocatalytic deactivation of TiO_2 film coated on ceramic substrate. *Journal of Physical Chemistry* 2007:9968–74.
52. Jung KY, Park SB. Effect of calcination temperature and addition of silica, zirconia, alumina on the photocatalytic activity of titania. *Korean Journal of Chemical Engineering* 2001;**181**:879–88.